Phase Diagram of Coacervate Complexes Containing Reversible Coordination Structures

ARTICLE *in* MACROMOLECULES · OCTOBER 2012

Impact Factor: 5.8 · DOI: 10.1021/ma301690t

Macromolecules

Article

pubs.acs.org/Macromolecules

Phase Diagram of Coacervate Complexes Containing Reversible Coordination Structures

Junyou Wang,* Martien A. Cohen Stuart, and Jasper van der Gucht

Laboratory of Physical Chemistry and Colloid Science, Wageningen University, Dreijenplein 6, 6703 HB Wageningen, The Netherlands

Supporting Information

ABSTRACT: Phase separation of coacervate complexes from cationic PDMAEMA [poly(*N*,*N*-dimethylaminoethyl methacrylate)] and anionic reversible coordination polymers are studied in the present work. The coordination polymers are formed from zinc and a bis-ligand L_2EO_4 [1,11-bis(2,6-dicarboxypyridin-4-yloxy)-3,6,9-trioxaundecane] and have variable chain length. The charge mixing ratio and metal-to-ligand ratio, M/L, are varied systematically, and the composition of the two coexisting phases is measured using ^{1}H NMR and ICP-AES. The resulting phase diagram is asymmetric: the coacervate complex phase tolerates an excess of coordination polymer much more than an excess of the homopolymer. Moreover, the coacervate complex tends to choose the right amount of the three components under nonstoichiometric mixing conditions. Both the metal-to-ligand ratio (M/L ≈ 1) and charge ratio ($f-$ ≈ 0.5) in the coacervate phase are around stoichiometry, leaving the excess components in the dilute phase.

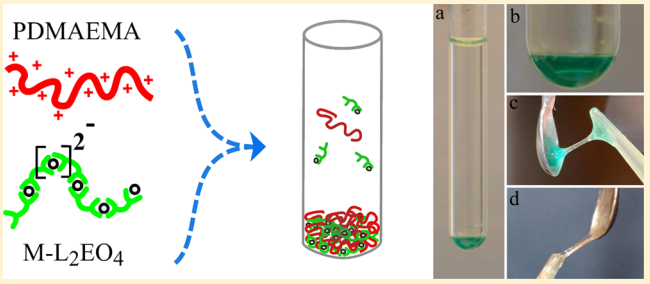

1. INTRODUCTION

Complex coacervation refers to the phase separation that occurs upon mixing oppositely charged polyelectrolytes in aqueous solution. Generally, the dilute phase contains mainly water and released counterions, while the concentrated phase is rich in both polyelectrolytes, which can be a precipitated solid complex or a liquid-like complex.[1,2] The latter was called a coacervate complex by Bungenberg de Jong and Kruyt, who were the first to investigate complexation in mixtures of gelatin and arabic gum.[3] The driving forces for complexation are the electrostatic attraction between polycations and polyanions and the entropy gain of the counterions that are released upon complex formation.[4,5]

In recent years, polyelectrolyte coacervates have been used to prepare nano- or microstructures as functional materials. For example, the macroscopic phase separation can be controlled into the colloidal domain by attaching a neutral hydrophilic block to one or both of the charged polymer chains, leading to formation of micelles with a complex coacervate core.[6] These micelles have been studied systematically by our group and some other groups.[7−9] Beside micelles, vesicles, microemulsions, hydrogels, brushes, and layer-by-layer structures based on coacervate complexes have been studied.[10−14] Despite this widespread use as a driving force, a fundamental understanding of complex coacervation is still lacking. The reason is that coacervate formation is a complicated process that depends on many factors, such as polymer chain length, charge density, polymer concentration, charge mixing ratio, ionic strength, pH, and temperature.[1,2] Overbeek and Voorn developed the first theoretical model for complex coacervation, in which they estimated the total free energy of mixing as the sum of the mixing entropy and the electrostatic interaction free energy from a Debye−Huckel approximation.[15] Based on this model, van der Gucht and co-workers reported a phase diagram for a system containing polycation and polyanion with equal charge and chain length.[5] Various improvements of the Voorn−Overbeek model have been reported, but a detailed comparison with experiment has not been made.[16−19]

Experimentally, a few studies have been carried out to investigate the phase diagram and the binodal compositions.[20−22] Chollakup et al. determined the phase boundaries between solution, coacervate, and precipitate for poly(acrylic acid) (PAA) and poly(allylamine hydrochloride) (PAH) mixtures, varying an extensive range of factors, including charge mixing ratio, polymer concentration, ionic strength, pH, and temperature.[1] Spruijt and co-workers studied the binodal compositions of coacervate complexes from poly(*N*,*N*-dimethylaminoethyl methacrylate) (PDMAEMA) and fluorescently labeled PAA.[2] The polymer chain length and salt concentration were mainly discussed in their work, but the mixing ratio was always equal to unity. All these studies are based on two oppositely charged polymers with equal chain length and charge. This makes the phase diagram symmetric with respect to an excess of either polycation or polyanion. In many cases, however, coacervate complexes from polyelectrolytes may be asymmetric in terms of chain length and charge

Received: August 9, 2012
Revised: October 8, 2012
Published: October 17, 2012

density. Early studies on such asymmetric polyelectrolyte complexes based on a long host polymer and shorter guest polymers with opposite charges were carried out by Tsuchida and Kabanov.[23−26] The shorter polyions were found to attach to part of the long polyion chains under nonstoichiometric mixing ratios to form soluble polyelectrolyte complexes with a neutralized domain. The structure, size and kinetics, and the effect of salt thereon were studied systematically, but no phase behavior and quantitative information about binodal compositions were included in these studies. Here, we make a new contribution to understand the phase separation of asymmetric polyelectrolyte mixtures. We study an extreme case, in which the polyanion is a supramolecular metal coordination polymer, which can adjust its molar weight distribution reversibly. Previously, we have shown that such coordination polymers can form complexes with polycation−neutral diblock copolymers, leading to metal-containing complex coacervate micelles. Here, we study bulk complexation with homopolyelectrolytes. We will show that the asymmetry between the two polyelectrolytes leads to a strong asymmetry in the phase diagram.

2. EXPERIMENTAL SECTION

2.1. Materials. Poly(*N*,*N*-dimethylaminoethyl methacrylate), PDMAEMA, was obtained from Polymer Source Inc. (M_w/M_n = 1.06, M_w = 17.0K, N = 108). The bis-ligand compound 1,11-bis(2,6-dicarboxypyridin-4-yloxy)-3,6,9-trioxaundecane (L_2EO_4) was prepared according to the literature.[27] $Zn(NO_4)_2{\cdot}4H_2O$, $NiCl_2{\cdot}6H_2O$ (analytical grade), 3-(trimethylsilyl)propanoic-2,2,3,3-d_4 acid sodium salt (TSP, 98% D), and deuterium oxide (99% D) were purchased from Aldrich and used without further purification.

2.2. Preparation of the Mixture. All the stock solutions were prepared in D_2O, and the pH was adjusted to 5 ± 0.2 with DCl or NaOD. The PDMAEMA at pH 5 is assumed to be protonated completely.[2] The mixing ratio between Zn-L_2EO_4 and PDMAEMA is presented as the mole fraction of negative charge, $f-$, which is defined as follows:

$$f- = \frac{[-]}{[-] + [+]} \quad (1)$$

where [−] and [+] are the molar charge concentrations of charged units on Zn-L_2EO_4 and PDMEAEMA. The positive charge fraction is $f+ = 1 - f-$. For mixtures at $f- < 0.5$, the concentration of PDMAEMA is fixed at 9.0 g/L, while Zn-L_2EO_4 increases from 0 to the charge stoichiometry. For mixtures at $f- > 0.5$, the coordination polymer concentration is fixed at 25.32 g/L and PDMAEMA is increased gradually. We kept the M/L at 1:1 (unless stated otherwise), the total volume at 4 mL, and the salt concentration (including counterions) at 0.1 ± 0.01 mM, adjusted with NaCl. For the mixtures with varying M/L ratios, the concentration of PDMAEMA was kept constant at 9.0 g/L, and either the amount of ligand or Zn^{2+} was doubled.

In a typical mixing procedure, ligand and PDMAEMA are mixed first, providing a transparent solution. Upon adding Zn^{2+} into the mixture, the solution becomes turbid immediately. The mixture was then shaken vigorously and sonicated for 10 min to mix well. After about 5 h, the solution became transparent again, and the polyelectrolyte complexes had sedimented to the bottom of the cell, either as solid precipitate or as liquid coacervate complexes. The phase-separated mixture was centrifuged gently at 3000*g* for 5 min after 3 days and then left to equilibrate further for another 3 days at room temperature. Both the dilute phase and the coacervate phase were transparent before analysis. To test whether the order in which the components are mixed plays a role, we have compared different mixing protocols for the sample prepared at $f- = 0.5$. In all cases, we found very similar compositions of the coexisting phases.

2.3. Analysis of the Separated Phases. The mixture separated into two clear phases after a few days. The top phase was transferred carefully with a graduated pipet, and its volume was determined. The concentrated phase was dissolved in D_2O containing 1 M NaCl. The two phases were both analyzed quantitatively with ^{1}H NMR to obtain the concentrations of PDMAEMA and L_2EO_4 and inductively coupled plasma atomic emission spectrometry (ICP-AES) to obtain the Zn^{2+} concentration.

The chemical structures of PDMAEMA and bis-ligand are shown in Scheme 1, and the characteristic protons for tracing polymer (amino groups) and ligand (pyridine ring) in ^{1}H NMR spectra are labeled with a star. The spectrum of the mixture of PDMAEMA and Zn−L_2EO_4 coordination polymers shows easily distinguished peaks for polymer and ligand, respectively (Supporting Information). With TSP [3-(trimethylsilyl)propanoic-2,2,3,3-d_4 acid sodium salt, 98% D] as quantitative internal standard, we then obtain the PDMEAEMA and ligand concentrations from the peak integrals. All the ^{1}H NMR measurements were carried out at 298 K on a Bruker AMX-400 spectrometer (400 MHz). The Zn^{2+} concentration in the two phases is determined by ICP-AES (Varian, Mulgrave, Australia). The complexes in solution need to be dissociated in advance. Typically, 0.5 mL of solution from the dilute or concentrated phase is added into 9.5 mL of 1.4 M HNO_3 solution, in which all the complexes in the mixture are assumed to be destroyed completely. For our method, the relative error in the calculated concentrations is estimated by summation of the relative errors from determining the volumes, weights of the components (1.6%), mixing ratio (2%), and integrals from ^{1}H NMR spectra (2%).

Scheme 1. (a, b) Structure of PDMAEMA and L_2EO_4;[a] (c) Illustration of Reversible Coordination Structures of M−L_2EO_4

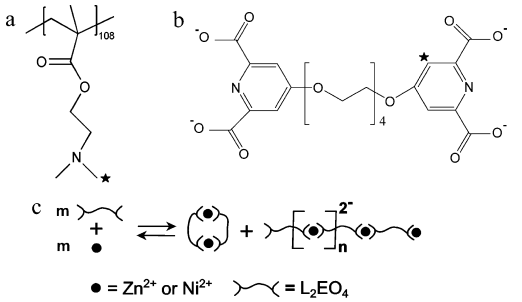

[a]The star signs represent the characteristic protons used for analyzing polymer and ligand in ^{1}H NMR spectra.

Dynamic light scattering (DLS) was used to characterize the coacervation process and structures of the polyelectrolyte complexes. The DLS measurement was performed with an ALV light scattering apparatus, equipped with a 400 mW argon ion laser operating at a wavelength of 532.0 nm. Measurements were done at a detection angle of 90° (corresponding to q = 22 247 820 m^{-1}), unless stated otherwise. All measurements were performed at room temperature. The size and size distribution are presented as the diffusion coefficient obtained from both CUMULANT and CONTIN methods.

3. RESULTS AND DISCUSSION

3.1. Observation of Phase Separation and Coacervate Complexes. The structure of Zn−L_2EO_4 coordination complexes has been studied systematically previously.[28] At a metal-to-ligand ratio M/L 1:1, the coordination complexes form small rings and short linear oligomers coexisting in the solution (Scheme 1). Both these structures are reversible and can change between each other, depending on the environmental factors. In general, the fraction of linear coordination polymers increases with increasing total concentration and temperature. In previous studies on complex coacervate core micelles formed with these coordination complexes, we found

dx.doi.org/10.1021/ma301690t | Macromolecules 2012, 45, 8903−8909

that micelles could be obtained even at very low concentration, where the coordination complexes in solution only form small rings and short oligomers.[29,30] However, in the absence of metal ions no micelles were formed, even though the free ligand molecules have more negative charges than the oligomers formed at M/L = 1.[29] This indicates that the cationic polymer chains must facilitate the growth of the coordination complexes into longer chains. The explanation that was given for this chain growth is that the coordination structures gather around the charged blocks during mixing, resulting in a high local concentration of the coordination complexes, enabling them to grow into longer linear structures.[31]

In the present study, the concentration of coordination complex is about 100 times higher than the concentration in the micellar systems. Upon mixing with oppositely charged PDMEAEMA, the Zn−L_2EO_4 coordination complexes are expected to form linear coordination polymers with negative charges distributed equally on the chain (Figure 1). In our

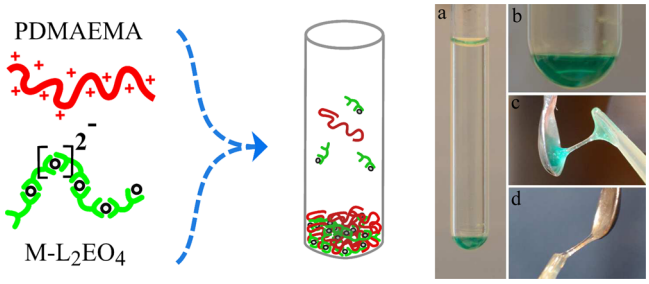

Figure 1. (left) Schematic illustration of the coacervate phase separation of PDMEAEMA and M−L_2EO_4 (M = Zn^{2+}, Ni^{2+}) mixture. (right) Pictures of the phase separation and coacervate complexes with Ni−L_2EO_4 (a, b, c) and Zn−L_2EO_4 (d) coordination polymers. M/L is fixed at 1/1, and charge mixing ratio (eq 1) *f*− is 0.5.

experiments, we found that mixing any two of the three components without the third one did not lead to phase separation, indicating that the complexation requires both electrostatic attraction and coordination.

Since Zn^{2+} ions are colorless, it is difficult to visualize the coacervate phase separation with Zn−L_2EO_4 complexes. As an alternative, we use Ni^{2+} as the metal ion, which gives the coacervate a green color. Two clear phases are shown in Figure 1a (M/L = 1/1, *f*− = 0.5). The top phase contains salt ions and a small amount of polyelectrolytes, so it is almost colorless. The bottom phase, by contrast, has a green color, indicating a high nickel concentration in the coacervate. The coacervate complexes are transparent, liquid-like but with a high viscosity, for the complexes from both the Ni−L_2EO_4 (Figure 1c) and Zn−L_2EO_4 (Figure 1d) coordination polymers. This gel-like appearance is quite similar to that of coacervate complexes formed by pure organic polyelectrolytes.[2]

3.2. Phase Diagram and Composition of the Complexes. Figure 2a shows the complex coacervate phase diagram that summarizes the binodal concentrations of PDMAEMA and Zn−L_2EO_4 in the dilute and concentrated phase at different charge mixing ratios. The overall M/L ratio is fixed at 1/1, and the salt concentration is controlled at 0.1 ± 0.01 M and assumed to be equal in both phases. The concentrations of PDMAEMA and Zn−L_2EO_4 polymers in the two phases are represented as the charge concentrations. Coexisting phases are connected by tie lines in the region where a liquid coacervate

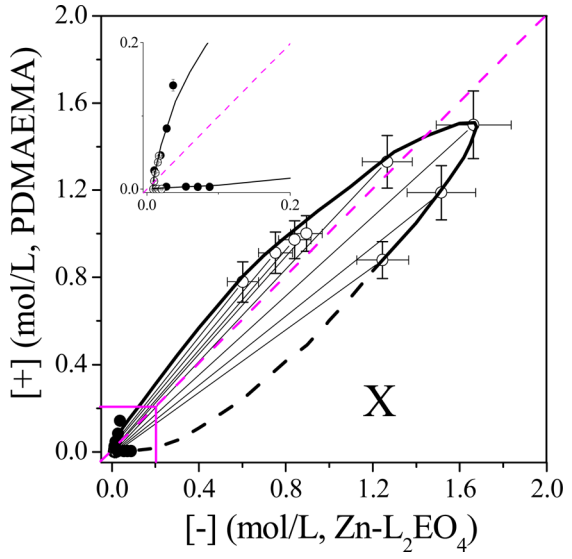

Figure 2. Phase diagram of the associative phase separation between PDMAEMA and Zn−L_2EO_4 coordination complexes (axes indicate concentrations of charges). The filled dots are the phase boundaries obtained from Figure 3. The magenta dashed line represents the charge stoichiometry, and the square indicates the range in which experiments were carried out. The inset is a magnification of the lower left region (low concentrations in dilute phase). In the region marked X, a solid precipitate is formed due to the limited solubility of the coordination polymer.

phase coexists with a dilute phase. Above this two-phase region, where there is an excess of polycation, there is only one phase which is a transparent solution. For excess coordination polymer, however, a solid precipitate is found when the amount of polycation is too low. Note that all these measurements are carried out for overall concentrations limited to the square area shown in Figure 2, since the coordination polymer is not soluble above 0.1 mol/L. The phase diagram is asymmetric: the two-phase region extends further below the diagonal dashed line that indicates charge stoichiometric mixing than above it. This means that the coacervate phase is more stable toward an excess coordination polymer than toward an excess of polycation. The Zn^{2+} and ligand concentrations in the two phases were measured separately, and all the Zn−L_2EO_4 coordination complexes in both top and coacervate phases have a M/L ratio around 1/1.

To estimate the phase boundary in the lower-left region of the phase diagram more precisely, we carry out titrations from two sides: adding PDMAEMA to a Zn−L_2EO_4 solution and the other way around. We first consider adding PDMAEMA to a Zn−L_2EO_4 coordination polymer solution (Figure 3a). At all the tested concentrations, adding PDMAEMA leads to precipitation if the positive charge fraction *f*+ exceeds a certain value, which varies from 4% to 10% with decreasing Zn−L_2EO_4 concentration. This part is indicated as S-L phase separation in Figure 3a. Apparently, the complexes formed under conditions of excess coordination polymer are poorly soluble. However, upon increasing the PDMAEMA concentration further, the complex phase becomes liquid, and we enter the liquid−liquid phase separation region. The phase boundary between the S-L and L-L regions is shown in Figure 2 as filled circles.

The situation is rather different for conditions of excess polycation. Adding Zn−L_2EO_4 coordination polymers to a PDMAEMA solution does not lead to phase separation until

dx.doi.org/10.1021/ma301690t | *Macromolecules* 2012, 45, 8903−8909

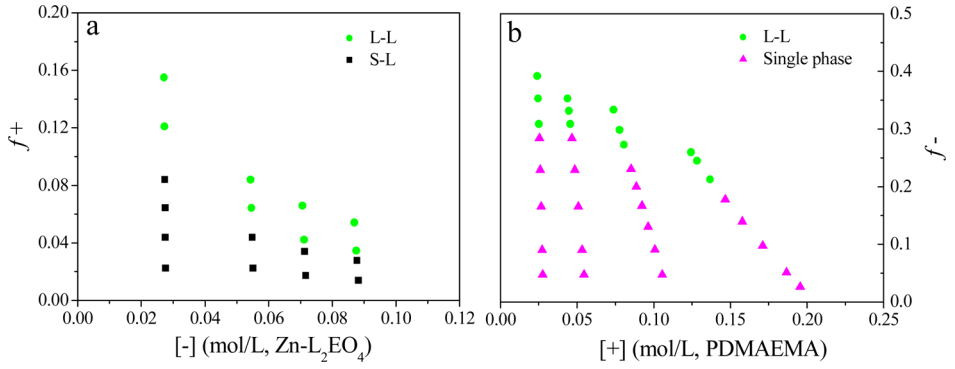

Figure 3. Phase boundaries determined by titration tests: (a) adding PDMAEMA to a $Zn-L_2EO_4$ solution; (b) adding $Zn-L_2EO_4$ to a PDMAEMA solution. The concentration of the component is represented as charge concentration. S-L: solid (precipitate)−liquid phase separation; L-L: liquid-like coacervate complexes separated from solution.

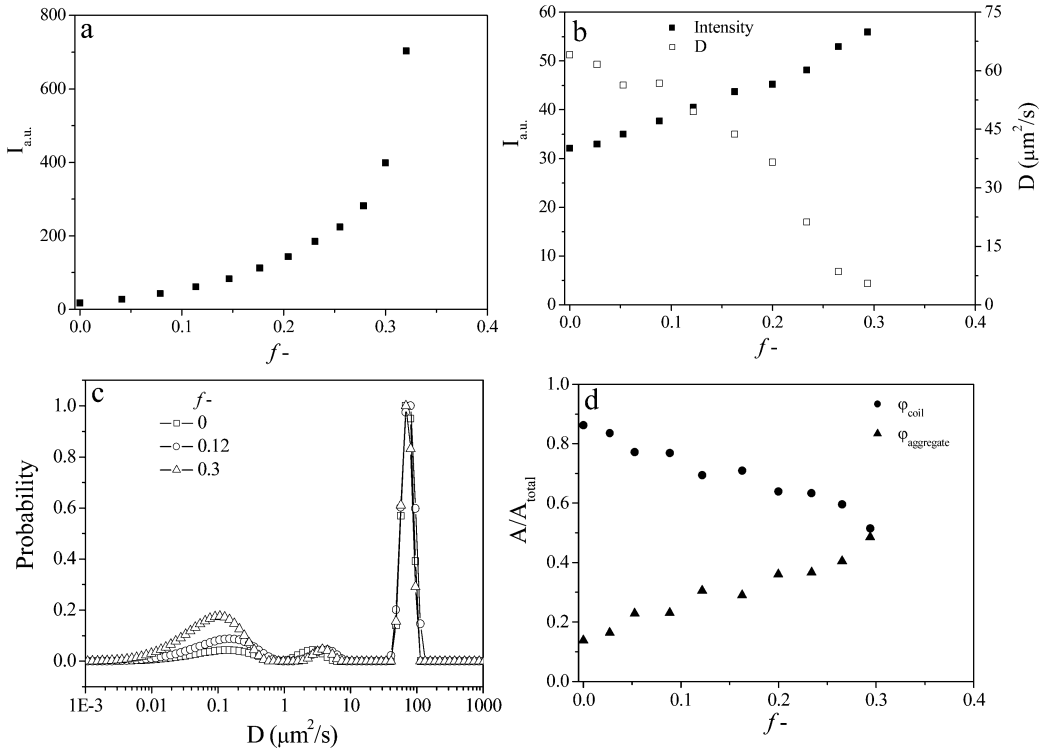

Figure 4. Variations of light scattering intensity and diffusion coefficient upon adding $Zn-L_2EO_4$ coordination complexes into PDMAEMA solution at $f-$ < 0.3. (a) $C_{PEMAEMA}$ 9 g/L. (b) $C_{PEMAEMA}$ 0.9 g/L. (c) CONTIN analysis of the size distribution of the titration performed at $C_{PEMAEMA}$ 0.9 g/L. (d) Contributions of the polymer coils and coil aggregates to the light scattering intensity, presented as the relative area fraction of the CONTIN peaks attributed to coil (D: 20−160 $\mu m^2/s$) and aggregates (D < 10 $\mu m^2/s$). Data in (c) and (d) were taken at a detection angle of 90°.

the fraction of negative charges $f-$ reaches ~0.3. Beyond this the solution is not stable. It first becomes turbid and then separates into two liquid phases after a few hours. From Figure 3a,b we see that liquid−liquid phase separation occurs roughly between $f-$ values between 0.3 and 0.9. This range becomes wider as the concentration increases. This means that it is more favorable to form liquid-like coacervate complexes at higher concentrations of the components.

What is the structure of the single-phase solution in the excess polycation region, at $f-$ < 0.3? We used DLS to characterize the titration process. Figure 4a shows the variation of the light scattering intensity upon adding $Zn-L_2EO_4$ to the PDMAEMA solution. The PDMAEMA concentration is 9 g/L. The intensity first increases gradually with increasing $Zn-L_2EO_4$ concentration and then shoots up at f_- ~ 0.3, confirming the phase boundary found in Figure 3b. At this high concentration, which is above the overlap concentration, it is not possible to determine the size of the formed complexes.[32] We therefore repeat the titration at a concentration which is 10 times lower. The polymer coils under this condition (0.9 g/L, pH 5, 0.1 ± 0.01 M) show a diffusion coefficient around 64 $\mu m^2/s$ (Figure 4b), which corresponds to a coil size of ~3 nm according to the Stokes−Einstein equation. The size increases with increasing $Zn-L_2EO_4$ amount, and big aggregates show up at $f-$ ~ 0.3. At the same time the light scattering intensity increases gradually. This indicates the formation of complexes already before the binodal composition is reached. In the studies of Tsuchida and Kabanov, soluble complexes formed if the long chain partly aggregated with short guest chains under nonstoichiometric mixing condition.[23−26] Here, similar struc-

dx.doi.org/10.1021/ma301690t | Macromolecules 2012, 45, 8903−8909

tures may be formed, in which the Zn−L_2EO_4 complexes partly decorate the cationic polymer chains, while the excess, uncompensated positive charges stabilize the complexes in solution. Only at higher concentrations of Zn−L_2EO_4, where most of the cationic charge is compensated, can the complexes aggregate to form a macroscopic coacervate phase.

CONTIN analysis shows two peaks in the distribution of diffusion coefficients (Figure 4c). We attribute the peak at diffusion coefficients between 20 and 160 $\mu m^2/s$ to partly decorated PDMAEMA coils and the peak at lower diffusion coefficient to large aggregates, consisting of aggregated complexes. As shown in the Supporting Information (Figure S1), the fast mode is independent of the wave vector q, while the apparent diffusion coefficient (Γ/q^2) of the slow mode increases with q. The latter is probably related to the polydispersity of the aggregates because large clusters contribute more at low q.[33] The relative contributions to light scattering intensity of these two kinds of objects are summarized in Figure 4d. Clearly, the number of partly decorated coils decreases, while the contribution of large aggregates increases with increasing Zn−L_2EO_4 amount.

The charge stoichiometry of the two different phases is shown in Figure 5. It is clear from this figure that the negative

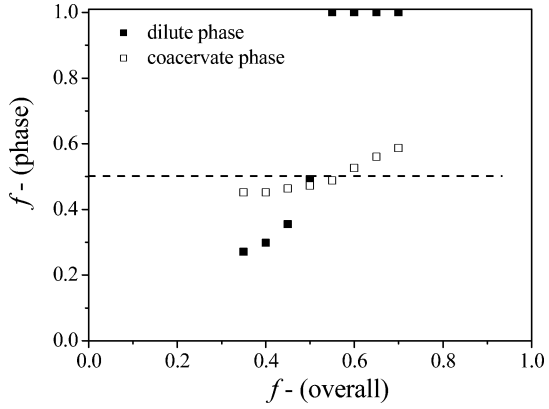

Figure 5. Charge fraction of Zn−L_2EO_4 coordination complexes in dilute phase and coacervate phase as a function of overall charge mixing ratio.

charge fraction in the dilute phase varies much more with the overall mixing ratio than the charge fraction in the coacervate phase, which remains around 0.5 for all the coacervate complexes formed with overall mixing ratio varying from 0.35 to 0.7. This means that the coacervate phase has a tendency to select a matching proportion between the charged components, while most of the excess components are expelled to the dilute phase. A similar selectivity has been reported in layer-by-layer structures containing Fe−L_2EO_4 coordination complexes, where they found that the coacervate multilayer always chose the charged components to match stoichiometry.[34]

Because of the selectivity of the coacervate phase, the dilute phase contains mostly the excess charged components if the overall charge ratio is not 0.5. The dilute solutions are analyzed with DLS, and the results are shown in Figure 6. At $f-$ > 0.5, excess Zn−L_2EO_4 complexes are in the dilute solution. The light scattering intensity is very low, indicating only soluble and small structures in the solution. This is consistent with previous findings that Zn−L_2EO_4 only forms small rings and short oligomers at low concentration without oppositely charged blocks.[28] On the other side, with excess of PDMAEMA in the

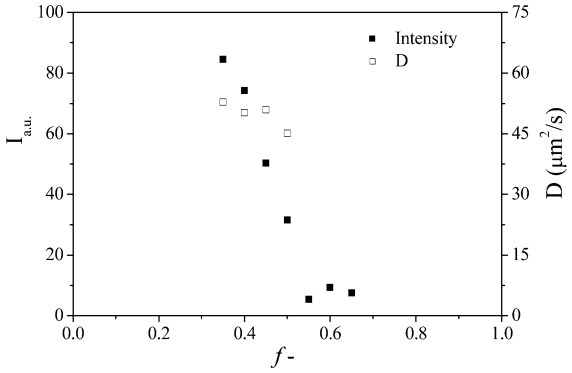

Figure 6. Light scattering analysis of the top solutions at different overall charge mixing ratio.

solution, we find soluble structures with a diffusion coefficient around 50 $\mu m^2/s$, which is similar to the size of PDMAEMA coils or partly decorated coils found when Zn−L_2EO_4 was added to the PDMAEMA solution at $f-$ < 0.3 (Figure 4b).

3.3. Composition of the Complexes with Varying M/L Ratio. Zn−L_2EO_4 coordination complexes respond not only to the overall concentration but also to the metal-to-ligand ratio, M/L. Long chains are only formed when the M/L ratio is close to 1.[28] At different ratios, either ligand or Zn^{2+} acts as a chain growth stopper, leading to shorter structures (see Scheme 2).

Scheme 2. Schematic Drawing of the Structure Changes of Zn−L_2EO_4 Coordination Complexes with Varying M/L

This is confirmed by viscosity measurements in previous studies.[28] In the present system, we also varied the M/L ratio to see whether this affects the complex coacervation process.

The PDMAEMA concentration is still fixed at 9 g/L, and either ligand or Zn concentrations are doubled. As shown in Figure 7a, the M/L ratio in the two phases responds differently to the overall M/L ratio. In the coacervate phase the M/L ratio deviates only slightly from 1/1 at all overall M/L ratios. By contrast, in the dilute phase, the M/L ratio changes dramatically upon varying the overall M/L ratio. The charge ratio, shown in Figure 7b, shows a similar dependence. This confirms that the coacervate phase indeed selects all the components around the right stoichiometry even when the overall M/L is not optimal for forming coordination polymers.

3.4. Asymmetry of the System. Upon mixing PDMAEMA and reversible Zn−L_2EO_4 coordination polymers in solution, we have found an asymmetric phase diagram: the coacervate phase tolerates excess coordination polymer better than excess polycation. This asymmetry arises because the coordination polymer can dissociate into smaller structures in the excess phase. As shown in Scheme 3, the dilute phase contains only a small amount of polyelectrolytes under charge stoichiometry ($f-$ 0.5). Upon increasing the amount of polycation ($f-$ < 0.5), the excess cationic polymers in the dilute phase attract more coordination complexes from the coacervate phase, which destabilizes the complex coacervate phase. Once the amount of polycation reaches the critical amount ($f-$ ~ 0.3), the coacervate phase disappears completely

dx.doi.org/10.1021/ma301690t | Macromolecules 2012, 45, 8903−8909

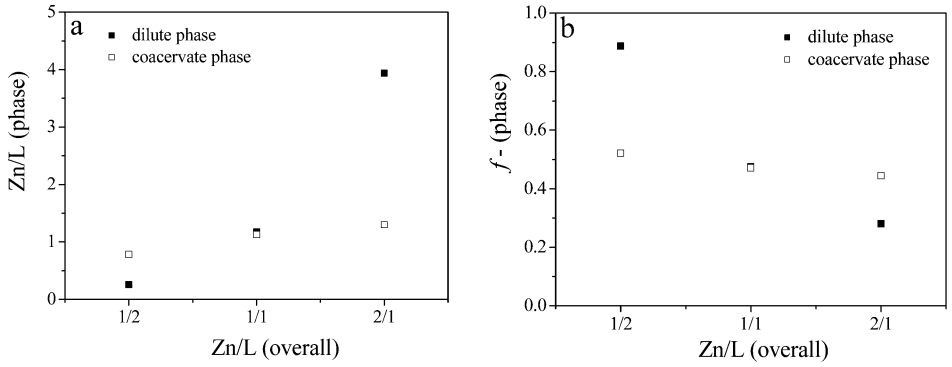

Figure 7. Zn/L ratio (a) and charge fraction (b) in the dilute and coacervate phases at different overall mixing M/L ratio.

Scheme 3. Schematic Illustration of the Asymmetry of Mixtures at Different Charge Mixing Ratios Represented as the Negative Charge Fractions[a]

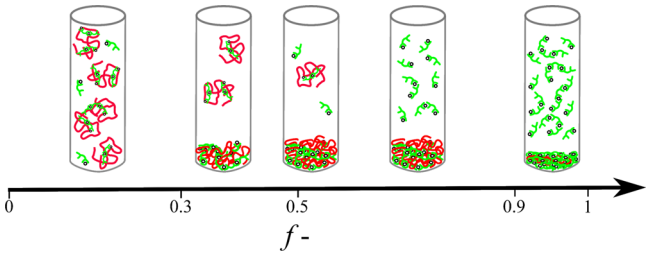

[a]Counterions and charges are not shown in the scheme.

and the two phases merge into one single phase, which contains soluble cationic polymer coils partly decorated with Zn−L_2EO_4 complexes. By contrast, an excess of coordination complexes does not affect the coacervate phase very much. The excess Zn−L_2EO_4 complexes in the dilute phase form only small structures in the absence of polycations. Apparently, these small structures are not strong enough to attract polycations into the dilute phase, so the coacervate phase remains stable in a wide range on this side ($f-$ 0.5−0.9). Only when the amount of coordination complexes is increased to $f- > 0.9$ does the liquid coacervate phase destabilize, forming poorly soluble complexes that sediment as a solid precipitate.

4. CONCLUSION

We have seen that coacervates of a cationic polymer and a reversible anionic coordination supramolecule have an asymmetric phase diagram: the coacervate complex phase tolerates an excess of coordination polymer much more than an excess of the homopolymer. This observation is completely different from coacervates in which the polycation and polyanion have an equal chain length and also an equal effect on coacervate stability. We believe that our result helps to understand asymmetric coacervation, which is more relevant for practical situations, since most coacervations in nature and in applications are based on asymmetric polyelectrolytes. Moreover, we found that the reversible nature of the coordination polymer helps the coacervate to select the right amount of the three components under nonstoichiometric mixing. Both the metal-to-ligand ratio (M/L ≈ 1) and charge ratio ($f- \approx 0.5$) in the coacerve phase are around the stoichiometry, and the excess components just stay in the dilute phase. This may help to simplify the procedure for preparing coacervate complexes, since the overall mixing ratio is not crucial anymore in asymmetric systems.

■ ASSOCIATED CONTENT

Supporting Information

^{1}H NMR spectra of L_2EO_4, Zn−L_2EO_4 complexes, PDMAEMA, and the total mixture with TSP as the internal standard; Figure S1. This material is available free of charge via the Internet at http://pubs.acs.org.

■ AUTHOR INFORMATION

Corresponding Author

*E-mail junyou.wang@wur.nl.

Notes

The authors declare no competing financial interest.

■ ACKNOWLEDGMENTS

The authors thank Barend van Lagen (Laboratory of Organic Chemistry, Wageningen University, Dreijenlaan 8, 6703 HB Wageningen, The Netherlands) for help with NMR experiments and Evan Spruijt (Laboratory of Physical Chemistry and Colloid Science, Wageningen University, Dreijenplein 6, 6703 HB Wageningen, The Netherlands) for the discussions about the experiment design and performance. We appreciate the help from Dmitry Ershov (Laboratory of Physical Chemistry and Colloid Science, Wageningen University, Dreijenplein 6, 6703 HB Wageningen, The Netherlands) with taking photos of the coacervate phase separation and complexes.

■ REFERENCES

(1) Chollakup, R.; Smitthipong, W.; Eisenbach, C. D.; Tirrell, M. *Macromolecules* **2010**, *43*, 2518−2528.
(2) Spruijt, E.; Westphal, A. H.; Borst, J. W.; Cohen Stuart, M. A.; van der Gucht, J. *Macromolecules* **2010**, *43*, 6476−6484.
(3) Bungenberg-de Jong, H.; Kruyt, H. *Proc. Sect. Sci., K. Ned. Akad. Wetenschappen* **1929**, *32*, 849−856.
(4) Dautzenberg, H. *Macromolecules* **1997**, *30*, 7810−7815.
(5) van der Gucht, J.; Spruijt, E.; Lemmers, M.; Cohen Stuart, M. A. *J. Colloid Interface Sci.* **2011**, *361*, 407−422.
(6) van der Burgh, S.; Cohen Stuart, M. A. *Langmuir* **2004**, *20*, 1073−1084.
(7) Voets, I. K.; de Keizer, A.; Cohen Stuart, M. A. *Adv. Colloid Interface Sci.* **2009**, *147−148*, 300−318.
(8) Harada, A.; Kataoka, K. *Macromolecules* **1995**, *28*, 5294−5299.
(9) Kabanov, A. V.; Bronich, T. K.; Kabanov, V. A.; Yu, K.; Eisenberg, A. *Macromolecules* **1996**, *29*, 6797−6802.
(10) Imura, T.; Yanagishita, H.; Kitamoto, D. *J. Am. Chem. Soc.* **2004**, *126*, 10804−10805.

(11) Hofs, B.; de Keizer, A.; van der Burgh, S.; Leermakers, F.; Cohen Stuart, M. A.; Millard, P. E.; Muller, A. *Soft Matter* **2008**, *4*, 1473−1482.
(12) Lemmers, M.; Sprakel, J.; Voets, I.; van der Gucht, J.; Cohen Stuart, M. A. *Angew. Chem., Int. Ed.* **2010**, *49*, 708−711.
(13) de Vos, W. M.; Kleijn, J. M.; de Keizer, A.; Cohen Stuart, M. A. *Angew. Chem., Int. Ed.* **2009**, *48*, 5369−5371.
(14) Tong, W.; Gao, C. Y. *J. Mater. Chem.* **2008**, *18*, 3799−3812.
(15) Overbeek, J.; Voorn, M. *J. Cell. Comp. Physiol.* **1957**, *49*, 7−26.
(16) Borue, V.; Erukhimovich, I. Y. *Macromolecules* **1990**, *23*, 3625−3632.
(17) Castelnovo, M.; Joanny, J.-F. *Langmuir* **2000**, *16*, 7524−7532.
(18) Popov, Y. O.; Lee, J.; Fredrickson, G. H. *J. Polym. Sci., Part B: Polym. Phys.* **2007**, *45*, 3223−3230.
(19) Lee, J.; Popov, Y. O.; Fredrickson, G. H. *J. Chem. Phys.* **2008**, *128*, 224908−1−224908−13.
(20) Zhang, R.; Shklovskii, B. I. *Physica A* **2005**, *352*, 216−238.
(21) Li, Y.; Dubin, P. L.; Havel, H. A.; Edwards, S. L.; Dautzenberg, H. *Langmuir* **1995**, *11*, 2486−2492.
(22) Wang, Y.; Kimura, K.; Dubin, P. L. *Macromolecules* **2000**, *33*, 3324−3331.
(23) Tsuchida, E.; Osada, Y.; Sanada, K. *J. Polym. Sci., Polym. Chem. Ed.* **1972**, *10*, 3397−3404.
(24) Tsuchida, E.; Osada, Y.; Ohno, H. *J. Macromol. Sci.* **1980**, *B17* (4), 683−714.
(25) Kabanov, V. A.; Zezin, A. B. *Sov. Sci. Rev., Sect. B: Chem. Rev.* **1982**, *4*, 207−282.
(26) Kabanov, V. A.; Zezin, A. B. *Pure Appl. Chem.* **1984**, *56*, 343−354.
(27) Vermonden, T.; Branowska, D.; Marcelis, A. T. M.; Sudholter, E. J. R. *Tetrahedron* **2003**, *59*, 5039−5045.
(28) Vermonden, T.; van der Gucht, J.; de Waard, P.; Marcelis, A. T. M.; Besseling, N. A. M.; Sudholter, E. J. R.; Fleer, G. J.; Cohen Stuart, M. A. *Macromolecules* **2003**, *36*, 7035−7044.
(29) Yan, Y.; Besseling, N. A. M.; de Keizer, A.; Marcelis, A. T. M.; Drechsler, M.; Cohen Stuart, M. A. *Angew. Chem., Int. Ed.* **2007**, *46*, 1807−1809.
(30) Wang, J. Y.; de Keizer, A.; Fokkink, R.; Yan, Y.; Cohen Stuart, M. A.; van der Gucht, J. *J. Phys. Chem. B* **2010**, *114*, 8313−8319.
(31) Yan, Y.; Besseling, N. A. M.; de Keizer, A.; Cohen Stuart, M. A. *J. Phys. Chem. B* **2007**, *111*, 5811−5818.
(32) Mckee, M. G.; Hunley, M. T.; Layman, J. M.; Long, T. E. *Macromolecules* **2006**, *39*, 575−583.
(33) Pusey, P. N.; van Megen, W. *J. Chem. Phys.* **1984**, *80*, 3513−3520.
(34) Lan, Y. R.; Xu, L. M.; Yan, Y.; Huang, J. B.; de Keizer, A.; Besseling, N. A. M.; Cohen Stuart, M. A. *Soft Matter* **2011**, *7*, 3565−3570.